Recent Great Lakes Evaporation Model Estimates

Thomas E. Croley II[1]

[1]Great Lakes Environmental Research Laboratory, National Oceanic and Atmospheric Administration, 2205 Commonwealth Blvd., Ann Arbor, Michigan 48105-2945; PH (734) 741-2238; FAX (734) 741-2055; email: Tom.Croley@noaa.gov

Abstract

NOAA's lumped-parameter Great Lakes continuous evaporation model solves for each day's over-water and over-ice surface fluxes (which in turn are functions of heat storage and ice and water surface temperatures). They include incident short-wave radiation, reflection, evaporative heat transfer (both latent and advected), sensible heat transfer, precipitation heat advection, long-wave radiation exchange, and surface flow advection. The model simultaneously finds daily heat storage and surface temperature with a heat balance, a model of linear temperature rise (or loss) with volume beneath the water surface, an empirical wind mixing model, and a one-dimensional (vertical) superposition of past aged heat additions or losses. The model couples ice formation and loss to lake thermodynamics and heat storage by utilizing both heat and mass balances for the ice pack and boundary conditions of ice-water existence. It simultaneously finds ice temperatures, pack size, and heat transferred between ice pack and both the atmosphere and the water.

Since measured whole-lake evaporation is unavailable, the model is calibrated to existing daily water surface temperatures and ice cover, and compared with measured temperature-depth profiles and independently estimated or measured water surface thermodynamic fluxes. Two calibrations are used to apply the model; the first minimizes error with observed water surface temperatures to determine parameters for superposition heat storage, wind mixing, and radiation exchange. The second minimizes error with observed ice cover to determine ice cover parameters. The calibrations alternate until changes in all parameters are insignificant. Presented calibrated parameters result in 1.1—1.6°C root mean square error with water surface temperatures and verify well over a time period independent of the calibration.

Example results of the evaporation model include estimated temperature-depth profiles over a year on Lake Michigan, and both a year's worth of daily evaporation and five years' worth of monthly evaporation on Lake Superior. Deep water evaporation characteristics are readily seen and described. Turnovers occur as a fundamental behavior of the model. Hysteresis between heat in storage and surface temperature, observed during the heating and cooling cycles on the lakes, is preserved. The model also correctly depicts lake-wide seasonal heating and cooling cycles, vertical temperature distributions, and other mixed-layer developments.

Over-Lake Evaporation Model

Great Lakes hydrological research mandates the use of continuous-simulation models of daily lake evaporation over long time periods. Such models must be usable in the

absence of water surface temperature and ice cover observations. They also must be physically based to have application under environmental conditions different than those under which they were derived. GLERL developed a lumped-parameter model of evaporation and thermodynamic fluxes for the Great Lakes based on an energy balance at the lake's surface (*Croley* 1989) and on one-dimensional (vertical) lake heat storage (*Croley* 1992). They coupled ice formation and loss also to lake thermodynamics and heat storage (*Croley and Assel* 1994). I describe the model here and apply it to Great Lakes data to summarize daily lake evaporation.

Thermodynamic Fluxes

The thermodynamic fluxes to and from a lake include incident short-wave radiation, usually taken as a linear function of cloud cover and short-wave radiation received on the Earth's surface under cloudless skies; see *Croley* (1989) for details of this and the following. Reflected short-wave radiation over water and ice is taken as a fraction of the incident, depending on incident angle and the water or ice surface condition. The latter includes snow condition. Evaporative heat transfer (both latent and advected) over water and ice, is calculated from the aerodynamic equation, which relates evaporation to the humidity difference between the overlying air and the water or ice surface and to wind speed. Sensible heat transfer over water and ice are calculated from the temperature difference between the overlying air and the water or ice surface and from wind speed. Precipitation heat advection over water and ice is estimated from rainfall or snowfall rates and air temperatures. Net long-wave radiation exchange is estimated from water temperature and the reflectivity and emissivity of water, as well as cloud cover. Finally, surface flow advection is estimated from lake inflows, outflows, and water temperatures.

Values of over-water and over-ice meteorology (humidity, wind speed, and air temperature) are determined from overland values by adjusting for over-water conditions. *Phillips and Irbe's* (1978) regressions for over-water corrections are used directly by replacing the fetch (and derived quantities) with averages. The bulk evaporation coefficients over water and over ice, used in estimating evaporation from humidity differences and wind speed, are determined similar to *Quinn* (1979) from over-water or over-ice (respectively) wind speed, air temperature, and surface temperature. The over-water and over-ice sensible heat coefficients, used in estimating sensible heat transfers from temperature differences and wind speed, are taken equal to the bulk evaporation coefficients, respectively. The emissivities of water and air and the reflectivity of the water surface are taken from *Keijman* (1974).

Only the net long-wave radiation is parameterized. By considering a water body as a "gray" body, and by applying cloud cover corrections only to counter-radiation from a clear sky (*Croley* 1989, equation 23),

$$Q_L = 5.67\times10^{-8}\left\{T_a^4\left(0.53+0.065\,e_a^{1/2}\right)\left[1+\left(p-1\right)N\right]-0.97\,T_w^4\right\}A \qquad (1)$$

where Q_L is daily net long-wave radiation exchange between the atmosphere and the water body (w), 5.67×10^{-8} is the Stefan-Boltzman constant (w m^{-2} $°K^{-1}$), T_a is air temperature (°K), e_a is vapor pressure of air (mb) at the 2-m height, p is an empirical

coefficient that reflects the effect of cloudiness on the atmospheric long-wave radiation to the water body (to be determined during a calibration of the model), N is cloud cover expressed as a fraction, 0.97 is emissivity of water, T_w is water temperature (°K), and A is lake surface area (m^2). When p is large, clouds return more of the lake's lost heat (the net effect is more heat in the lake) then when p is small.

Heat Storage

The heat added to a lake and the heat added to the ice pack, from the surface fluxes, are governed by simple energy and mass balances, energy-storage relationships, and boundary conditions on ice growth, water temperature, and ice temperature. The heat addition during a day, ΔH, is given from accounting of all surface fluxes:

$$\Delta H = \left[A_w \left(q_i - q_r - q_e + q_h + q_p \right) + Q_L + Q_I - Q_w \right] \times 1 \text{ day} \qquad (2)$$

where A_w is the open water surface area (m^2), q_i, q_r, q_e, q_h, and q_p are the daily rates of, respectively, incident, reflected, evaporative (latent and advected), sensible, and precipitation-advected heat to the water surface (w m^{-2}), Q_I is surface flow advection (w) and Q_w is total heat flux between the water body and the ice pack (w). The latter is found by joint solution with the ice balance equations, presented subsequently.

Croley (1989) applied the mixed-layer concept of others (*Gill and Turner* 1976; *Kraus and Turner* 1967) for the Great Lakes. Spring turnover (convective mixing of deep cold low-density water with cool high-density surface waters) occurs when surface temperature increases to 3.98°C, the temperature for maximum density of water. As water temperatures begin increasing above 3.98°C, surface temperature increases faster than temperatures at depth, developing a stable temperature-depth profile with warmer, lower-density waters on top. As the net heat flux to the surface then changes to negative, surface temperature drops and convective mixing keeps an upper layer at uniform temperature throughout (the "mixed layer"). The mixed layer deepens with subsequent heat loss until the temperature is uniform over the entire depth at 3.98°C, representing fall turnover. Then a symmetrical behavior is observed with temperatures less than 3.98°C as the lake continues to lose heat; temperature drops more on the surface than at depth until the net surface flux changes to positive again. Surface temperature then increases toward 3.98°C, and convective mixing forces uniform temperature at all depths, representing spring turnover.

Consider heat additions for water temperatures above 3.98°C, after spring turnover has occurred. During the day, a heat addition, ΔH, penetrates a water volume, M, near the surface, referred to as the "mixing volume" attributable to ΔH. The addition raises water temperatures throughout the mixing volume and the water temperature increase, Δt, is taken as linear with volume, v, measured down from the lake surface; see Figure 1. It varies from its maximum, $\Delta t = \Delta T$ at the surface (v= 0), to $\Delta t = B$ at the bottom of the mixing volume ($v = M$). Volume M subsequently increases (deepens) with time as a function of conduction, diffusion, and mechanical (wind) mixing and, in a sufficiently large lake, approaches a limiting value (an "equilibrium volume," V_e) since the effects of wind mixing at the surface diminish with distance from the surface. While M is increasing, ΔH mixes throughout M until, at some volume (M

= F), ΔH becomes fully mixed (temperature rise constant with depth). If a fully-mixed condition does occur at some point, then $F < V_e$. As M grows from its initial value to F, the surface water temperature rise, ΔT, decreases with increased mixing of ΔH throughout M and also with increases in M. The temperature rise at the bottom of the mixing volume, B, also would increase with the mixing of ΔH but the increase in M would decrease it. Therefore, B is taken as constant until ΔH is fully mixed throughout (when $M = F$). Thus, B corresponds to the fully mixed condition ($M = F$) where the temperature-rise at any depth, Δt, is constant throughout M: $\Delta t = \Delta T = B = \Delta H / (\rho_w C F)$. (Here ρ_w = density of water and C = specific heat of water.) See Figure 1. As M grows beyond F ($M \geq F$), the temperature rise profile remains uniform (fully mixed), but the (spatially constant) water temperature increment, B, decreases.

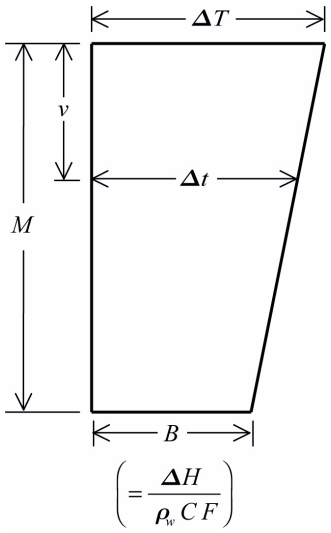

Figure 1. Temperature rise profile.

The above considerations apply equally well to heat losses ($\Delta H < 0$) and water temperature decreases, but with a different value for the fully mixed volume (F'). Large F (after spring turnover) or F' (after fall turnover) result in larger surface temperature differences, than do small F or F', and steeper temperature gradients. Thus heat is distributed vertically more uniformly for small values of F or F' than for large.

Note that the assumed temperature *rise*profile (not the *temperature* profile) is assumed to be linear until the fully mixed condition obtains. This is not the same as assuming that the temperature profile is linear; indeed the epilimnetic temperature profile will behave like the mixed-layer model already discussed.

Wind Mixing and Superposition

As mentioned above, M increases with time as a function of wind mixing. There should be some nonzero volume for no accumulated wind movement (accumulated wind movement equals zero), and the mixing volume should approach the limiting equilibrium volume V_e (in a sufficiently large lake) as the accumulated wind movement increases. *Croley* (1992) studied empirical relationships with these characteristics and suggested an exponential form relating M and accumulated average wind-days over the water surface:

$$M_{k,m} = V_e \Big/ \left[1 + a \exp\left(-b \sum_{j=m}^{k} w_j \right) \right] \tag{3}$$

where $M_{k,m}$ is size of the mixing volume on day k associated with the heat added on day m, w_j is average wind speed on day j, and a and b are empirical coefficients. Equation (3) applies for the post spring turnover period (water temperatures are greater than 3.98°C); its counterpart for the post fall turnover period (water temperatures are less than 3.98°C) has the same form but the coefficients are a' and b'.

Note that for large V_e, surface temperature differences are distributed more quickly at depth than for small V_e, all other things being equal. The parameters *a* or *a'* determine the "no wind" mixing of surface temperature changes. As *a* or *a'* increase, "no wind" mixing approaches 0, and as *a* or *a'* decrease (toward zero), it approaches V_e. The parameters *b* or *b'* determine the effect of wind on the mixing volume of a heat addition or deletion, for water temperatures above or below 3.98°C, respectively. As *b* or *b'* increase, the wind effect on mixing is more pronounced and $M_{k,m} \rightarrow V_e$ more quickly, thus more quickly distributing surface temperature changes at depth. As *b* or *b'* decrease, the wind effect on mixing is less pronounced.

Extending *Kraus and Turner's* (1967) mixed-layer thermal structure concept to determine simple heat storage, the above assumptions and definitions are combined into a heat superposition model. Each day it combines temperature rise profiles and temperature drop profiles from all past surface heat additions or deletions. Effects of past heat additions or losses thus are superimposed to determine surface temperature on any day as a function of heat in storage; each past addition or loss is parameterized by age. It adjusts when instability exists in the form of higher-density waters overlying lower-density waters (colder water above warmer when both are above 3.98°C or warmer water above colder when both are below 3.98°C). The adjustment redistributes heat so that the total temperature is uniform with depth (volume) over the region of the instability. Turnovers (convective mixing of deep lower-density waters with surface waters as surface temperature passes through that at maximum density) can occur as a fundamental behavior of this superposition model and hysteresis between heat in storage and surface temperature, observed during the heating and cooling cycles on the lakes, is preserved. Noting that ΔH is just the difference between total stored heat in the lake, *H*, on successive days, water surface temperature becomes:

$$T_k = 3.98°\text{C} + \sum_{m=1}^{k} f_{k,m} \left(\underset{m \le n \le k}{\text{MIN}}\ H_n - \underset{m-1 \le n \le k}{\text{MIN}}\ H_n \right) \tag{4}$$

where T_k is water surface temperature and H_k is heat storage in the lake *k* days after the last turnover, and $f_{k,m}$ is a "wind-aging" function relating surface temperature rise on day *k* to heat added on day *m*. The "wind-aging" function, $f_{k,m}$, is:

$$\begin{aligned} f_{k,m} &= \frac{2 - M_{k,m}/F}{\rho_w C_w M_{k,m}}, && M_{k,m} < \text{MIN}\left(F,\ \frac{2V_c}{1+V_c/F} \right) \\ &= \frac{1}{\rho_w C_w M_{k,m}}, && \text{MIN}\left(F,\ \frac{2V_c}{1+V_c/F} \right) \le M_{k,m} < \text{MAX}\left(V_c,\ \frac{2V_c}{1+V_c/F} \right) \\ &= \frac{1}{\rho_w C_w V_c}, && \text{MAX}\left(V_c,\ \frac{2V_c}{1+V_c/F} \right) \le M_{k,m} \end{aligned} \tag{5}$$

where V_c = volume (capacity) of the lake. Parameters *a*, *b*, *F*, (and *a'*, *b'*, *F')* and V_e are empirical parameters found by calibrating to observations. *Croley* (1992) derives (4) and (5), including the entire temperature-depth profile each day from superposition principles.

Ice Pack Growth

The time rate of change of heat storage in the ice pack, *dH'/dt*, is:

$$\frac{dH'}{dt} = A\left(q_i - q_r' - q_e' + q_h' + q_p'\right) + Q_w \tag{6}$$

where the prime notation on the surface fluxes denotes "over-ice". The heat storage change both alters ice temperatures [ice temperature is taken as linear from surface to 0°C at bottom (*Green and Outcalt* 1985)] and freezes or melts ice. No ice exists if water surface temperature exceeds 0°C and temperature is 0°C if ice exists; Q_w is chosen appropriately. Q_w, if negative, is yielded as ice forms (to keep water temperature at 0°C) and, if positive, is used in melting ice (to keep water temperature at 0°C as long as there is ice present). Ice surface temperature is taken equal to over-ice air temperature if ice exists and air temperature is at or below 0°C; it is taken as 0°C if over-ice air temperature exceeds 0°C. Ice pack, *V*, changes with new ice, *V'*, freezing or melting, snow fall, *S*, and ice evaporation, *E*:

$$\frac{dV}{dt} = \frac{dV'}{dt} + S - E \tag{7}$$

The heat exchange between the atmosphere and the ice pack, available for freezing or melting, is taken as resulting in either melt (along the entire atmosphere-ice surface) or freezing (along the entire water-ice surface). The heat exchange between the water body and the ice pack, Q_w, is taken as resulting in changes along only the water/ice surface (either melt or freezing). *Croley and Assel* (1994) solved (6)—(7) simultaneously with the surface flux relations and heat superposition already mentioned. The solution contains two empirical coefficients, τ_a and τ_w, to be determined in a calibration. They relate to ice pack shape, number of ice pack pieces, the ratios of vertical to lateral changes along the atmosphere-ice interface and along the water-ice interface, respectively, and the buoyancy of ice. Large values of τ_a or τ_w, imply that there are many pieces of ice, resulting in a large combined edge surface relative to the lateral ice surfaces (top or bottom); large values also imply more effective heat transfer through vertical ice surfaces (ice pack edge) relative to the lateral surfaces.

Application

Two calibrations are used to apply the model. The first determines the first eight parameters (*a*, *b*, *F*, *a'*, *b'*, *F'*, V_e, and *p*). The first seven parameters relate to superposition heat storage (*Croley* 1992) and the eighth parameter, *p*, reflects the effect of cloudiness on the atmospheric net long-wave radiation exchange (*Croley* 1989). This calibration minimizes daily surface temperature root mean square error (RMSE) by systematically searching the parameter space. The second calibration determines the two parameters (τ_a and τ_w) that minimize daily ice cover RMSE. Ice cover parameters are held constant during the first calibration and the superposition and radiation parameters are held constant during the second. The calibrations alternate until the RMSEs for both water surface temperatures and ice cover do not significantly reduce.

Prior to calibration or model use, the (spatial) average temperature-depth profile in the lake and the ice cover must be initialized. While the ice cover is known as zero during major portions of the year, the temperature-depth profile in the lake is difficult to determine. If the model is used in forecasting or short simulations, then we must determine these variables accurately prior to model use. If used for calibration or for long simulations, then initial values are generally unimportant. Their effect diminishes with time, and after 2-3 years of simulation, they are practically nil.

Meteorology data (air temperature, wind speed, humidity, and cloud cover) for 1948-2003, generally observed at airports, were available from the Ontario Climatic Center, Environment Canada, and the US National Climatic Data Center. Daily synoptic observations were Thiessen-averaged to determine areal meteorological time series over each of the lake surfaces. Water surface temperatures on each Great Lake, except Lake Michigan, were taken from airplane and satellite measurements, extended through August 1988, and prepared as described by *Croley* (1989). Water surface temperatures for Lake Michigan from 1981 through 1985 were gleaned from areal maps prepared at the National Weather Service's Marine Predictions Branch and extended through August 1988 also. Lake-averaged ice cover for model calibration was extracted from GLERL's ice cover databases (*Assel* 1983; *Assel and Norton* 2001).

Table 1 summarizes calibrated parameters and Great Lake statistics. Table 2 depicts statistics of calibration and independent verification. There is good agreement between actual and calibrated-model water surface temperatures; the RMSE is between 1.1-1.6°C on the large lakes (within 1.1-1.9°C for an independent verification period). The RMSE for ice concentrations is between 12 and 23% for the joint calibration-verification period. There is also good agreement with 8 years of bathythermograph observations of depth-temperature profiles on Lake Superior and 1 year of independently derived weekly or monthly surface flux estimates on Lakes Superior, Erie, and Ontario (2 estimates) (*Croley* 1989, 1992). Turnovers occur as a fundamental behavior of GLERL's thermodynamic and heat storage model; see the example in Figure 2. Hysteresis between heat in storage and surface temperature, observed dur-

Table 1. Lake Evaporation and Thermodynamics Model Constants and Parameters.

	Lake					
	Superior	Michigan	Huron	Georgian	Erie	Ontario
Area, km^2	82,100	57,800	40,640	18,960	25,700	18,960
Volume, km^3	12,100	4,920	2,761	779	484	1,640
Depth, m	147	85.1	67.9	41.1	18.8	86.5
a	$6.298\times10^{+0}$	$7.290\times10^{+0}$	$6.460\times10^{+0}$	$1.585\times10^{+0}$	$2.820\times10^{+0}$	$7.710\times10^{+0}$
b, m^{-1} s	3.298×10^{-3}	2.599×10^{-3}	2.810×10^{-3}	5.473×10^{-3}	5.430×10^{-3}	2.800×10^{-3}
F, km^3	$3.273\times10^{+3}$	$5.100\times10^{+2}$	$4.890\times10^{+3}$	$1.101\times10^{+3}$	$1.000\times10^{+2}$	$2.000\times10^{+2}$
a'	$2.019\times10^{+0}$	$1.158\times10^{+0}$	$3.829\times10^{+0}$	$1.471\times10^{+0}$	$2.610\times10^{+0}$	$4.000\times10^{+0}$
b', m^{-1} s	3.795×10^{-3}	2.301×10^{-3}	3.890×10^{-3}	1.103×10^{-2}	5.600×10^{-3}	5.110×10^{-3}
F', km^3	$5.113\times10^{+3}$	$4.000\times10^{+3}$	$6.789\times10^{+3}$	$8.943\times10^{+2}$	$1.000\times10^{+2}$	$4.600\times10^{+2}$
Ve, km^3	$1.200\times10^{+4}$	$5.006\times10^{+3}$	$8.010\times10^{+3}$	$9.748\times10^{+2}$	$8.490\times10^{+2}$	$2.000\times10^{+3}$
p	$1.299\times10^{+0}$	$1.068\times10^{+0}$	$1.150\times10^{+0}$	$1.223\times10^{+0}$	$1.290\times10^{+0}$	$1.200\times10^{+0}$
τ_a	$9.011\times10^{+8}$	$9.001\times10^{+8}$	$9.119\times10^{+8}$	$9.279\times10^{+8}$	$9.988\times10^{+8}$	$9.010\times10^{+8}$
τ_w	$8.002\times10^{+5}$	$2.003\times10^{+5}$	$1.080\times10^{+6}$	$4.437\times10^{+5}$	$9.202\times10^{+5}$	$8.001\times10^{+4}$

Table 2. Lake Evaporation and Thermodynamics Model Calibration Statistics.

	Lake					
	Superior	Michigan	Huron	Georgian	Erie	Ontario
CALIBRATION PERIOD STATISTICS						
Water Surface Temperatures (1980-1988)						
Means Ratio	1.00	1.01	0.98	1.01	1.03	0.99
Variances Ratio	1.01	0.98	0.95	1.02	1.08	0.99
Correlation	0.98	0.97	0.98	0.99	0.99	0.98
RMSE, ºC	1.13	1.56	1.33	1.10	1.58	1.43
Ice Concentrations (1960-1988)						
Means Ratio	0.92	0.72	0.70	0.98	1.15	0.39
Variances Ratio	1.24	1.02	1.67	1.62	1.09	0.63
Correlation	0.76	0.83	0.73	0.77	0.89	0.54
RMSE, ºC	23.4	12.4	26.0	21.5	19.0	15.4
VERIFICATION PERIOD STATISTICS						
Water Surface Temperatures (1966-1979)						
Means Ratio	0.96		1.03	0.98	1.05	0.94
Variances Ratio	1.10		0.95	1.00	1.10	0.97
Correlation	0.97		0.99	0.98	0.98	0.96
RMSE, ºC	1.09		1.10	1.34	1.91	1.92

ing the heating and cooling cycles on the lakes, is preserved. The model also correctly depicts lake-wide seasonal heating and cooling cycles, vertical temperature distributions, and other mixed-layer developments.

Great Lakes Evaporation Estimates

The model is applied to historical meteorological data starting in 1948; Figure 3 shows excerpts from the simulation for Lake Superior. The 1995 daily plot reveals much of the structure of deep lake evaporation throughout the year. The time-occurrence structure of evaporation on the Great Lakes suggests correspondence with air mass movements over the lakes; large amounts of the annual evaporation total appear to occur over small portions of the year on an event-oriented basis. Note that most of the evaporation occurs during the winter when the lake is warmest relative to the overlying air and the air is very dry. This is due to the very large thermal inertia of the lake, associated with the large lake heat storage, which causes water temperatures to lag air temperatures during the annual cycle. There is small negative evaporation in the summer, corresponding to condensation onto the lake surface when the lake surface is cooler than the overlying air. The 1991—1995 monthly plot in Figure 3 illustrates typical interannual variation of Lake Superior.

Discussion and Summary

A heat storage superposition model is described that explicitly considers lake capacity and mixing capacity in temperature-depth profile development as a function of the

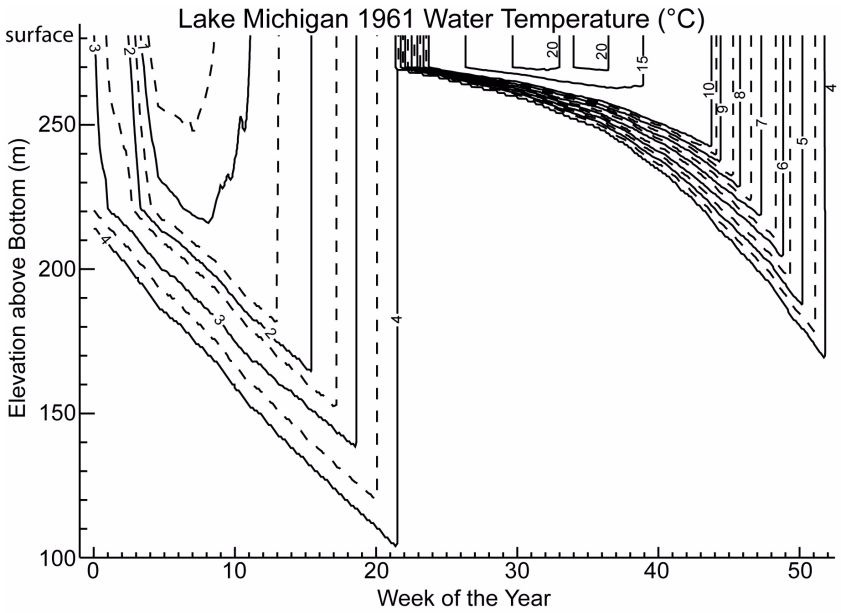

Figure 2. Estimated 1961 Michigan Temperature Profiles.

wind-aging of past heat additions. This conceptual model depicts seasonal heating and cooling cycles, heat-temperature hysteresis, water column turnovers, and mixed-layer developments, in accordance with other investigators' physical models, while providing the capability for multiple, long-period, continuous simulations. We can now look at continuous long-term dynamics of lake heating and evaporation; this enables further studies of climate change, water balances, groundwater, ice, lake-effect snowfall, and other evaporation-dependent phenomenon.

The most serious shortcoming of this model relates to the multi-dimensional nature of the ice formation and loss process. This is indicated by a model bias toward over-estimation of the number of winters without ice cover and in general toward under-estimation of ice cover. The boundary condition that prohibits ice growth until the average water surface temperature reaches freezing, is responsible for this under-estimation. Instead, the surface temperature and heat storage in same-depth segments of the lake could be considered in bathymetry-weighted calculations to allow ice formation in the segments as surface temperatures reach freezing. This represents an extension of the existing areal point model in one or more spatial dimensions.

The ice sub-model theory also could be improved by including ice break-up and re-joining mechanisms related to wind, melting, and refreezing. However, a trial formulation resulted in an over-specified model for the data sets currently at hand, and the additional parameters were indeterminate. Other improvements include formulation of a snow-cover layer on the ice, parameterization of surface (ice and snow) albedo in terms of daily meteorological inputs, and consideration of the effects of solar radiation absorption by ice and snow on ice strength and albedo. It is doubtful if these or other improvements in model theory would add significantly to accuracy in this one-dimensional formulation since extensive data on the spatial and temporal extent of snow on ice are unavailable at present for the Great Lakes. Lateral heating, cooling, and momentum transfer at the lakes surface are not adequately addressed in a one-

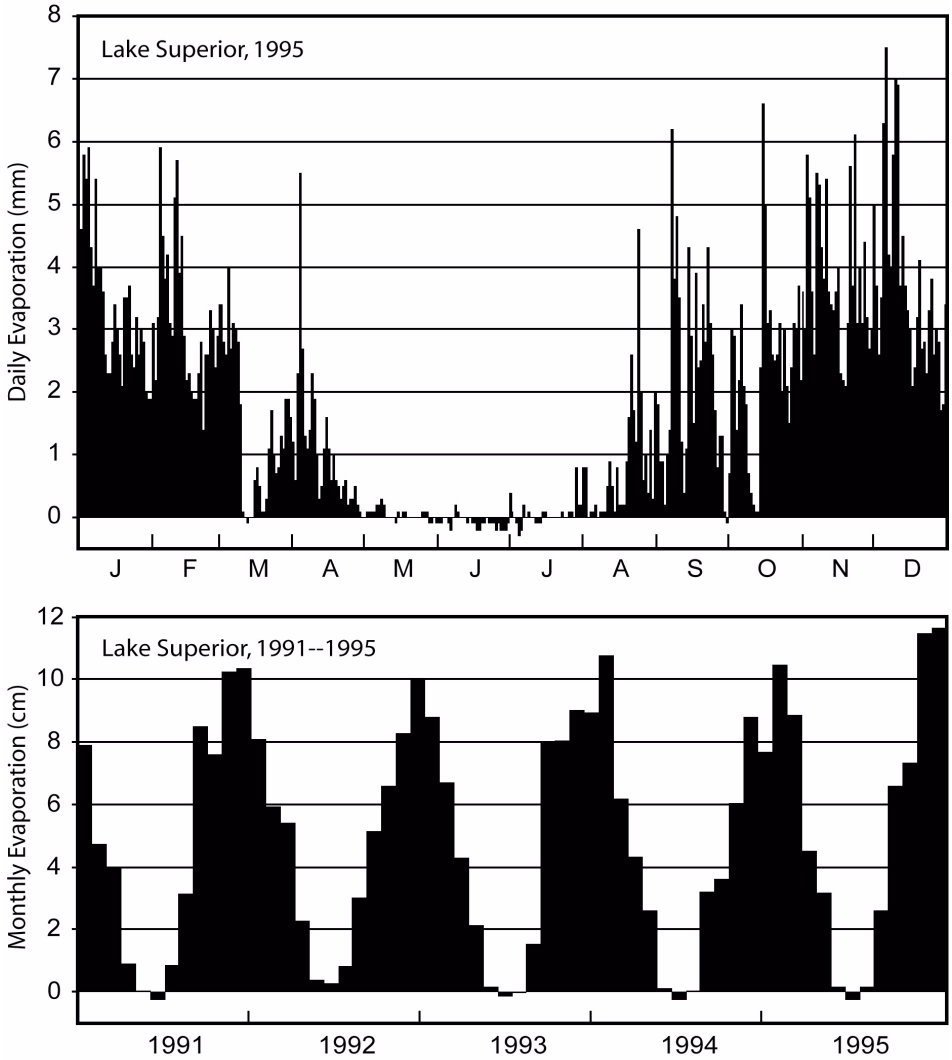

Figure 3. Estimated Lake Superior Evaporation Examples.

dimensional model. This tended to be less of a problem on Lake Erie because of its much smaller average depth. However, even on Lake Erie, the effects of winds, currents, and ice movement on lake-averaged ice cover were not adequately addressed.

Acknowledgments

This is GLERL contribution no. 1342.

References

Assel, R. A., 1983. A computerized data base of ice concentration for the Great Lakes. *NOAA Data Report ERL GLERL-24*, Great Lakes Environmental Research Laboratory, Ann Arbor, Michigan.

Assel, R.A. and D.C. Norton, 2001. Visualizing Laurentian Great Lakes ice cycles, *EOS Transactions of the American Geophysical Union*, **82**(7).

Croley, T. E., II, 1989. Verifiable evaporation modeling on the Laurentian Great Lakes. *Water Resource Research*, **25**(5):781-792.

Croley, T. E., II, 1992. Long-term heat storage in the Great Lakes. *Water Resources Research*, **28**(1):69-81.

Croley, T. E., II, and R. A. Assel, 1994. A one-dimensional ice thermodynamics model for the Laurentian Great Lakes. *Water Resources Research*, **30**(3):625-639.

Gill, A. E., and J. S. Turner, 1976. A comparison of seasonal thermocline models with observation, *Deep Sea Research*, **23**:391-401.

Green, G. M., and S. I. Outcalt, 1985. A simulation model of river ice cover thermodynamics. *Cold Reg. Sci. & Technol.*, **10**:251-262.

Keijman, J. Q., 1974. The estimation of the energy balance of a lake from simple weather data. *Boundary-Layer Meteorology*, **7**:399-407.

Kraus, E. B., and J. S. Turner, 1967. A one-dimensional model of the seasonal thermocline II; the general theory and its consequences. *Tellus*, **19**:98-105.

Phillips, W. D., and J. G. Irbe, 1978. Land-to-lake comparison of wind, temperature, and humidity on Lake Ontario during the International Field Year for the Great Lakes (IFYGL). *Report CLI-2-77*, Environment Canada, AES, Downsview.

Quinn, F. H., 1979. An improved aerodynamic evaporation technique for large lakes with application to the International Field Year for the Great Lakes. *Water Resources Research*, **15**(4):935-940.